

## The effects of motion on the dose distribution of proton radiotherapy for prostate cancer

Sima Qamhiyeh,<sup>1a</sup> Dirk Geismar,<sup>1</sup> Christoph Pöttgen,<sup>2</sup> Martin Stuschke,<sup>1,2</sup> Jonathan Farr<sup>1</sup>

*Westdeutsches Protonentherapiezentrum Essen,<sup>1</sup> Essen, Germany; Klinik für Strahlentherapie,<sup>2</sup> Universitätsklinikum Essen, Essen, Germany  
Sima.Qamhiyeh@uk-essen.de*

Received 30 March, 2011; accepted 19 December, 2011

Proton radiotherapy of the prostate basal or whole seminal vesicles using scattering delivery systems is an effective treatment of prostate cancer that has been evaluated in prospective trials. Meanwhile, the use of pencil beam scanning (PBS) can further reduce the dose in the beam entrance channels and reduce the dose to the normal tissues. However, PBS dose distributions can be affected by intra- and interfractional motion. In this treatment planning study, the effects of intra- and interfractional organ motion on PBS dose distributions are investigated using repeated CT scans at close and distant time intervals. The minimum dose ( $D_{\min}$ ) and the dose to 2% and 98% of the volumes ( $D_{2\%}$  and  $D_{98\%}$ ), as well as EUD in the clinical target volumes (CTV), is used as measure of robustness. In all patients,  $D_{98\%}$  was larger than 96% and  $D_{2\%}$  was less than 106% of the prescribed dose. The combined information from  $D_{\min}$ ,  $D_{98\%}$  and EUD led to the conclusion that there are no relevant cold spots observed in any of the verification plans. Moreover, it was found that results of single field optimization are more robust than results from multiple field optimizations.

PACS numbers: 87.55.D-, 87.55.de, 87.53.Bn, 87.55.dk, 87.55.ne

Key words: prostate cancer, treatment planning, particle therapy, robustness, retrospective study

### I. INTRODUCTION

Locally advanced prostate cancers show a strong dose-response relationship. Proton radiotherapy to the prostate and basal or whole seminal vesicles with a dose up to 82 Gy<sub>1,1</sub> was found effective and tolerable in retrospective and prospective trials.<sup>(1-3)</sup> Gy<sub>1,1</sub> is the dose in units of Cobalt equivalent doses assuming a radiobiological effect of 1.1.<sup>(4)</sup> The above clinical studies were performed with classic double scattering proton therapy systems. Compared to intensity-modulated radiation therapy (IMRT), double scattering proton techniques result in better distributions of the low and intermediate dose region to the surrounding organs at risk. The proton dose distributions are similar or better in the high-dose region, depending on the lateral penumbra of the proton beam.<sup>(5-6)</sup> The applied dose distributions have similar dependencies on interfractional anatomic motions as dose distributions by IMRT.<sup>(7)</sup> According to existing planning studies,<sup>(8-10)</sup> intensity-modulated proton radiotherapy (IMPT) using pencil beam scanning techniques (PBS) can further improve the dose distributions achieved by passively scattered protons, and can give superior dose distributions than current IMRT techniques. However, inter- and intrafractional motion might affect PBS dose distributions to larger extent.<sup>(10-12)</sup>

This paper is a retrospective study which is carried out with repeated planning CT scans to estimate the effect of intra- and interfractional organ motion on the resulting dose distribution.

<sup>a</sup> Corresponding author: Sima Qamhiyeh, Westdeutsches Protonentherapiezentrum Essen, Hufelandstrasse 55, 45147 Essen, Germany; phone: +49 (0)201 723 4746; fax: +49 (0)201 723 5169; email: Sima.Qamhiyeh@uk-essen.de

It focuses on intermediate- to high-risk prostate cancer treatment using PBS. In the study, the target volume coverage and dose to the organs at risk were assessed for four different treatment planning setups. In contrast to a robustness study which focuses only on interfractional motion effects,<sup>(12)</sup> the present study distinguishes between intra- and interfractional motion, and analyses the effects on dose distribution in clinical prostate cases.

## II. MATERIALS AND METHODS

All patients who were considered for the study have been treated with either 3D conformal or IMRT between December 2008 and March 2009 at our institution. Before their treatment, the patients received a planning CT (CT-A1) and two low-dose CTs (CT-A2 and CT-A3). The CTs were taken five minutes (CT-A2) and ten minutes (CT-A3) after the reference planning CT (CT-A1) and during the same immobilization session. A second planning CT (CT-B1) was taken on a second day. The scan protocol used for the low-dose CTs is identical to the one used for planning CT, except that the mAs used for low-dose CT is ~30% of the mAs used for the planning CT. The calibration of CT numbers to electron density was the same for both planning and low dose CTs. The multiple CTs were performed to construct the internal target volume of the prostate and seminal vesicles by comparing the different planning CTs using gold markers implanted into the prostate or intraprostatic calcifications. Image guidance by internal prostate markers can effectively decrease the effect of interfractional motion on the coverage of the target by the dose distribution.<sup>(11,13-14)</sup> The only selection criterion was that all patients had internal prostate markers used for patient repositioning. This resulted in a heterogeneous group of patients in terms of patient positioning aid. In a subset of the patients, where calcifications in the prostate were observed, the calcifications were used as internal markers. In the remaining patients, radio-opaque prostate implants were implanted at least one week before the first planning CT. The patients were immobilized in the supine position using either a body form or a knee-foot fixation. The patients were also instructed to empty their bladder and rectum one hour before the acquisition of the CT, and to drink 350 ml of water. In some patients, rectal balloons were used to reduce rectal toxicity and enhance prostate immobilization.<sup>(15-16)</sup> The interfractional displacement of the prostate can be considerably high as a result of using the endorectal balloon.<sup>(17)</sup> A rectal balloon (Rüsch AG, Kernen, Germany) of 7 cm length and a 75 ml maximum volume capacity and 30 cm long catheter was used during this study. The heterogeneous patient group was useful to demonstrate the application of the beam arrangements on a variety of clinical conditions.

The clinical target volumes (CTVs), the planning target volumes (PTVs), and the critical organs at risk (OARs) were delineated based on recommendations of the EORTC Radiation Oncology Group.<sup>(18)</sup> For this planning study, two CTV structures were delineated for each patient: CTV1 and CTV2. CTV1 represented the prostate and bilateral seminal vesicles with a margin of up to 0.5 cm around the prostate but not across anatomic borders (i.e., muscles at the outer rectal wall). CTV2 represented the prostate and proximal seminal vesicles within the first 0.5–1.0 cm. These CTVs were compatible with the RTOG0415 protocol on IMRT for prostate cancer, and the results of internal motion studies after online correction using implanted markers by Meijer et al., van der Wielen et al., and Kotte et al.<sup>(19-21)</sup> In this study, the PTVs were created by expanding the respective CTVs by 0.8 cm around the seminal vesicles and 0.5 cm around the prostate.

The dose prescriptions were 60 Gy<sub>1,1</sub> for PTV1. An additional 18 Gy<sub>1,1</sub> was prescribed for PTV2. The summed dose will add to 78 Gy<sub>1,1</sub> in the prostate. The treatment planning constraints listed in Table 1 include minimum dose ( $D_{\min}$ ), average dose ( $D_{\text{mean}}$ ), maximum dose ( $D_{\max}$ ), dose to a relative volume such as  $D_{98\%}$ , and volume at given doses (Gy<sub>1,1</sub>) such as  $V_{82}$  which could be extracted from the dose volume histograms (DVH). All patients had to fulfill all the constraints in Table 1 in all plans. The dose was to be delivered in 2 Gy<sub>1,1</sub> fractions. It

TABLE 1. Treatment planning constraints: dose volume constraints which should be fulfilled by all initial treatment plans performed on the CT-A1 for CTVs and OARs.

| Volume    | Dose Constraints ( $Gy_{1,1}$ ) |           |             |                    | %Volume Constraints at Given Dose ( $Gy_{1,1}$ ) |           |           |           |           |           |           |           |           |
|-----------|---------------------------------|-----------|-------------|--------------------|--|-----------|-----------|-----------|-----------|-----------|-----------|-----------|-----------|
|           | $D_{min}$                       | $D_{max}$ | $D_{mean}$  | $D_{98\%}-D_{2\%}$ | $V_{82}$   | $V_{80}$  | $V_{75}$  | $V_{70}$  | $V_{65}$  | $V_{60}$  | $V_{50}$  | $V_{40}$  | $V_{18}$  |
| CTV1      | 60.0                            | -         | -           | -                  | -  | -         | -         | -         | -         | -         | -         | -         | -         |
| CTV2      | 18.0                            | -         | -           | -                  | -  | -         | -         | -         | -         | -         | -         | -         | -         |
| PTV1      | 48.0                            | 72.0      | $\leq 63.0$ | $\leq 7.2$         | -  | -         | -         | -         | -         | $\geq 95$ | -         | -         | -         |
| PTV2      | 14.4                            | 21.6      | $\leq 18.9$ | $\leq 2.2$         | -  | -         | -         | -         | -         | -         | -         | -         | $\geq 95$ |
| Rectum    | -                               | -         | -           | -                  | -  | $\leq 2$  | $\leq 12$ | $\leq 20$ | $\leq 30$ | $\leq 45$ | $\leq 50$ | $\leq 70$ | -         |
| Bladder   | -                               | -         | -           | -                  | $\leq 2$   | $\leq 12$ | $\leq 20$ | $\leq 30$ | $\leq 45$ | -         | $\leq 60$ | -         | -         |
| Left Hip  | -                               | 45.0      | -           | -                  | -  | -         | -         | -         | -         | -         | -         | -         | -         |
| Right Hip | -                               | 45.0      | -           | -                  | -  | -         | -         | -         | -         | -         | -         | -         | -         |

was estimated that the time required to deliver the dose is ten minutes per fraction. Only one fraction would be delivered per day. The dose planned for PTV1 (60  $Gy_{1,1}$ ) would be delivered first, followed by PTV2 (18  $Gy_{1,1}$ ).

IMPT plans were calculated on CT-A1 using Varian Eclipse software version 8.6 (Varian Medical Systems, Palo Alto, CA). The isocenter was chosen to be the volumetric center of the prostate, as calculated from the prostate markers. A virtual machine with PBS abilities and an initial beam sigma of 0.4 cm in air was used. The spot spacing in and between scanning layers was 0.5 cm. The grid size used for the calculation was  $0.25 \times 0.25 \times 0.25 \text{ cm}^3$ . For each of the patients, four plan arrangements were considered. In this study, each plan consisted of two fields: Bi-lateral ( $90^\circ$  and  $270^\circ$ ) and lateral-oblique ( $85^\circ$  and  $275^\circ$ ). The different beam angulations were considered to avoid beam paths parallel to interfaces of density changes as would be expected if the axis connecting the femur head and the greater and lesser trochanter structures is parallel to the proton beam. No distal modifications were performed to compensate for setup errors or range uncertainties. For each field arrangement, single field optimization (SFUD) and multiple field optimization (MF) were tested. The option of the field optimization technique was used as offered in the plan setup mode of the treatment planning system. To summarize, a bilateral MF (LMF), an oblique MF (OMF), a bilateral SFUD (LSF), and an oblique SFUD (OSF) treatment plans were calculated for each patient in this study. The dose to the different structures was analyzed using DVH parameters and generalized equivalent uniform dose (EUD)<sup>(22)</sup> to help identify cold spots.<sup>(23)</sup> EUD was evaluated as  $EUD = \left[ \frac{1}{N} \sum_i^N (d_i)^\alpha \right]^{1/\alpha}$ , where  $i$  was the voxel of interest which receives a dose  $d_i$ ,  $N$  was the total number of voxels,  $\alpha$  was the tissue specific volume parameter.  $\alpha$  of -10 was chosen for EUD calculation of the prostate.<sup>(6,24-25)</sup>

The effect of geometrical changes on dose distribution in the CTV and the OAR were analyzed separately for intra- and interfractional motion type. To analyze the effect of intrafractional motion on dose distribution, the treatment plans were recalculated on CT-A2 and CT-A3. Assuming that the patients will be perfectly positioned at the beginning of the first treatment fractions, CT-A1, CT-A2, and CT-A3 can be considered as snapshots of patient anatomy at the beginning, half way, and at the end of a treatment fraction, respectively. Intrafractional interplay effects and anatomical changes between fields within a fraction were not analyzed. The interplay between position of spots of a PBS field and anatomical changes is beyond the scope of this work.

In analyzing interfractional motion, the dose is recalculated on the CT-B1 which was registered to CT-A1 using bony landmarks. Then, the field's isocenter was readjusted to match the volumetric center of the prostate as calculated from the prostate markers. The correction in the position of the isocenter was equivalent to translational setup corrections of patient position between fractions.

CTV coverage was considered the criterion for plan robustness. A plan was deemed robust if the minimum dose in CTVs was more than 90% of the prescribed dose (54.0 Gy<sub>1,1</sub> for CTV1 and 70.2 Gy<sub>1,1</sub> for CTV2) in CT-A2, CT-A3, and CT-B1. Meanwhile, the effect of change in patient anatomy on the dose to the OAR was analyzed using DVH parameters.

### III. RESULTS

Table 2 shows the different setups of patient immobilization and the consequent inter- and intrafractional motion. Looking at the changes in bony anatomy, two distinct patterns of motion can be distinguished. One is the translation and rotation of the pelvic girdle. The other is the rotation of the femur. The position of the femoral heads is fixed with respect to the pelvic girdle even when a rotation of the femur is observed. However, such a rotation results in a change in the alignment of the femoral neck and the adjacent greater and lesser trochanter structures. The quantification of changes in bony anatomy is not trivial. From the data, one out of six patients (17%) who were immobilized with the half body forms showed intrafractional motions of the bony anatomy. In comparison, three out of four patients (75%) in the knee-foot fixation showed change in the bony anatomy intrafractionally. Interfractionally, change in bony anatomy happens in higher frequency in patients with knee-foot fixation (50%) vs. patients in the form (33%).

In two out of three patients who received a rectal balloon, changes exceeding 0.5 cm in the position of the balloon were observed in the repeated CTs (see Table 2). The Table also summarizes measured change in bladder volume in different CTs relative to CT-A1 where a positive change indicates increase in bladder volume.

In Table 3, the change in position of the prostate relative to CT-A1, calculated from the internal markers, is shown for all three directions: Left-Right (LR), Anterior-Posterior (AP) and Cranio-Caudal (CC). Furthermore the amplitude of the 3D vector is also calculated.

All initial treatment plans (optimized based on CT-A1) fulfilled the treatment planning criteria in Table 1 in terms of CTV and PTV coverage, as well as OAR sparing. An exception was the fourth patient for whom the PTV2 enclosed 11% of the rectal volume. There, it was geometrically impossible to fulfill the  $V_{75}$  constraint in that case. Comparing the bilateral plans with the oblique field arrangement (OMF vs. LMF and OSF vs. LSF) and comparing multiple field optimization vs. single field optimization (LMF vs. LSF and OMF vs. OSF), no significant

TABLE 2. Summary of intra- and interfractional motion of the study patients. The reported values are all relative to the initial planning CT (CT-A1). If no value is given, the observed change was less than 3 mm.

| Patient Index | Immobilization Setup | Change in Bony Anatomy     | Presence of Rectal Balloon | Change in                                     |                         |                         |                                      |
|---------------|----------------------|----------------------------|----------------------------|---|-------------------------|-------------------------|--------------------------------------|
|               |                      |                            |                            | Rectal Balloon Position in CT-B1 <sup>a</sup> | Bladder Volume in CT-A2 | Bladder Volume in CT-A3 | Bladder Volume in CT-B1 <sup>b</sup> |
| 1             | Form                 |                            | No                         |   | 18%                     | 45%                     | 9%                                   |
| 2             | Form                 | Interfractional            | No                         |   | 0%                      | 0%                      | -15%                                 |
| 3             | Form                 | Interfractional            | No                         |   | 4%                      | 7%                      | -67%                                 |
| 4             | Form                 |                            | No                         |   | 8%                      | 18%                     | -15%                                 |
| 5             | Knee-foot            |                            | No                         |   | 6%                      | 10%                     | -5%                                  |
| 6             | Knee-foot            | Intra- and Interfractional | No                         |   | 12%                     | 27%                     | -38%                                 |
| 7             | Knee-foot            | Intra- and Interfractional | No                         |   | 10%                     | 34%                     | -75%                                 |
| 8             | Form                 |                            | Yes                        | -1.0 cm                                       | 0%                      | 11%                     | 93%                                  |
| 9             | Knee-foot            | Intrafractional            | Yes                        |   | 12%                     | 27%                     | -21%                                 |
| 10            | Form                 | Intrafractional            | Yes                        | +3.5 cm                                       | 8%                      | 20%                     | 23%                                  |
| Average ± SD  |                      |                            |                            |   | 8±6%                    | 20±14%                  | -11±48%                              |

<sup>a</sup> The changes in position of rectal balloon are reported only along the crania-caudal direction.

<sup>b</sup> Summary of the average ± standard deviation of the change in bladder volume.

TABLE 3. Change in position of the prostate as calculated from the internal markers relative to CT-A1; all values are presented in cm. The amplitude of the 3D vector is also shown, along with the average and standard deviations (SD).

| Patient Index | CT-A2 |      |      |           | CT-A3 |      |      |           | CT-B1 |      |      |           |
|---------------|-------|------|------|-----------|-------|------|------|-----------|-------|------|------|-----------|
|               | LR    | AP   | CC   | 3D Vector | LR    | AP   | CC   | 3D Vector | LR    | AP   | CC   | 3D Vector |
| 1             | 0.0   | 0.1  | 0.0  | 0.1       | -0.1  | 0.1  | 0.0  | 0.1       | -0.1  | -0.1 | -0.2 | 0.2       |
| 2             | 0.1   | 0.2  | 0.0  | 0.2       | 0.0   | -0.1 | -0.1 | 0.1       | 0.0   | 0.3  | -0.1 | 0.3       |
| 3             | -0.1  | -0.1 | 0.2  | 0.2       | 0.0   | -0.2 | 0.2  | 0.2       | 0.0   | -0.1 | 0.1  | 0.1       |
| 4             | 0.1   | 0.0  | 0.2  | 0.2       | 0.1   | -0.1 | 0.3  | 0.3       | 0.0   | -0.3 | 0.3  | 0.4       |
| 5             | 0.0   | -0.4 | 0.5  | 0.6       | 0.0   | -0.2 | 0.2  | 0.3       | -0.2  | -0.6 | 0.7  | 0.9       |
| 6             | -0.1  | 0.2  | -0.4 | 0.4       | 0.1   | 0.2  | -0.3 | 0.4       | -0.6  | -0.3 | 0.3  | 0.8       |
| 7             | 0.0   | -0.1 | -0.1 | 0.1       | 0.0   | 0.2  | -0.3 | 0.3       | 0.1   | 0.0  | 0.2  | 0.2       |
| 8             | -0.1  | -0.1 | -0.2 | 0.2       | 0.2   | 0.2  | -0.3 | 0.4       | 0.1   | -0.1 | -0.2 | 0.2       |
| 9             | 0.1   | 0.0  | 0.2  | 0.2       | 0.0   | -0.1 | 0.0  | 0.1       | -0.1  | -0.6 | 0.5  | 0.8       |
| 10            | 0.1   | -0.2 | 0.3  | 0.4       | 0.0   | -0.7 | 0.3  | 0.8       | 0.2   | -0.6 | 0.2  | 0.7       |
| Average       | 0.0   | 0.0  | 0.1  | 0.3       | 0.0   | -0.1 | 0.0  | 0.3       | -0.1  | -0.2 | 0.2  | 0.5       |
| SD            | 0.1   | 0.2  | 0.3  | 0.2       | 0.1   | 0.3  | 0.2  | 0.2       | 0.2   | 0.3  | 0.3  | 0.3       |

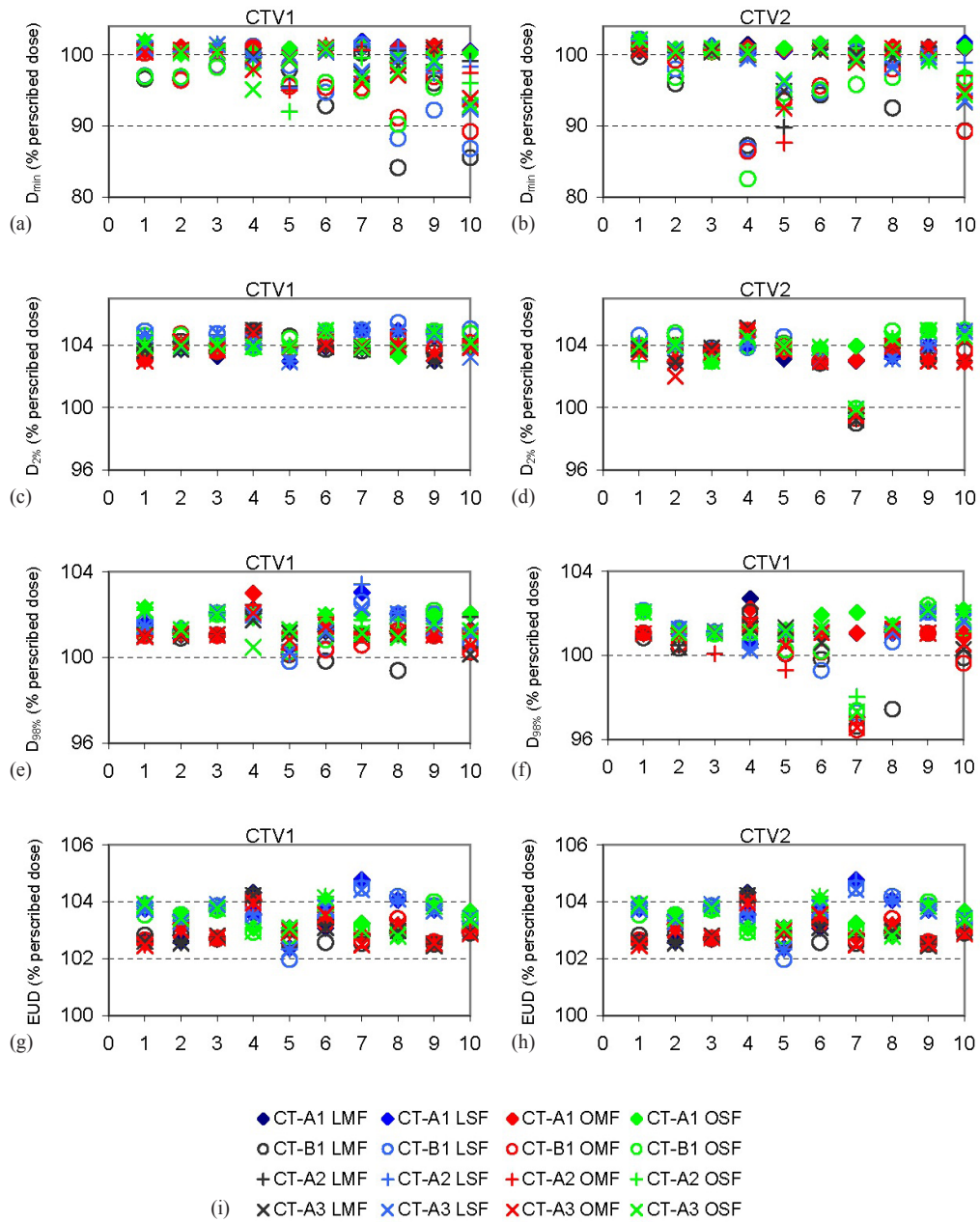
LR = Left–Right; AP = Anterior–Posterior; CC = Cranio–Caudal.

changes in the EUD of CTVs was observed. The EUD was always 2.5%–3.5% higher than the prescribed dose. Similarly,  $D_{\min}$ ,  $D_{98\%}$  and  $D_{2\%}$  showed little variation due to selection of planning technique for the initial treatment plans. Effects due to changes in patient anatomy were most prominent in  $D_{\min}$  compared to the other parameters (see Fig. 1).

As for robustness,  $D_{\min}$  in CTVs was more than 90% of the prescribed dose in CT-A2, CT-A3 (intrafractionally), and CT-B1 (interfractionally) in most patients (see Fig. 1). All plans of all patients are robust with respect to intrafractional motion, except for the fifth patient. In that case, the position of the prostate varied by a 3D vector of 0.6 cm. The LSF and OSF plans were above the 90% constraint and, therefore, robust. Interfractionally, patient 4 fails the criterion on  $D_{\min}$  with all modalities. However, no major motion patterns were detected interfractionally in the case of patient 4. Upon close inspection, the CTV2 volume which received 100% of the prescribed dose ( $V_{100\%}$ ) was found to vary between 99.8% and 99.9% suggesting that only 0.1%–0.2% of the voxels were represented by  $D_{\min}$  values. Patients 8 and 10 are not robust to interfractional motion. In both cases, the rectal balloon was used, but the balloon was not placed at the same position as in CT-A1. Nonetheless, both LSF and OSF techniques for patient 8 and the OSF of patient 10 were still robust. Meanwhile, the near minimum value ( $D_{98\%}$ ) is above the 96% and the near maximum ( $D_{2\%}$ ) is less than 106% for all patients (see Fig. 1).  $D_{98\%}$  appears insensitive to the changes in anatomy compared to  $D_{\min}$ .

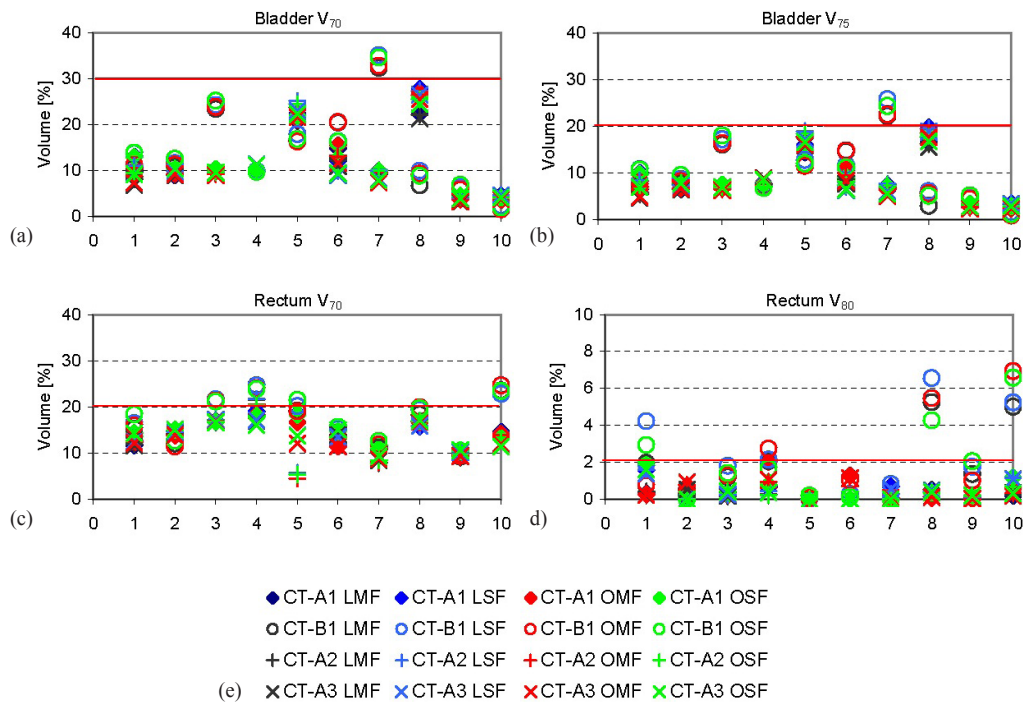
For bladder and rectum, Fig. 2 displays some of the controlled volume parameters on CT-A1 and the verifications on CT-A2, CT-A3, and CT-B1. Logically, an increase in the volume causes a reduction of the measured dose parameters. For most patients, bladder dose-volume parameters are far beyond the tolerance values set in Table 1 for the initial treatment plans. The values are within tolerance for all intrafractional verifications. In the case of the 7th patient, a reduction of the bladder volume by 75% led to exceeding the tolerance on  $V_{70}$  and  $V_{75}$  in all interfractional verifications.

For rectal dose parameters, the fourth patient was the only patient for which rectal doses exceeded the tolerances intrafractionally. Interfractionally, in the cases where the repositioning of a smaller rectal balloon of 50 ml was performed, rectal balloons showed a large variation —  $V_{80}$  was 2–4 fold the accepted tolerance volume of 2%. These changes were also reflected on  $D_{\min}$  of CTV1 for both patients 8 and 10. Smaller effects were seen in CTV2 (see Fig. 1).



Note: The x-axis of the graphs is the patient index as listed in Table 2. Plans on CT-A1 are referred to with full simples; the interfractional verifications on CT-B1 are indicated by circles; the intrafractional verifications on CT-A2 and CT-A3 are shown as plus (+) and cross (x) signs, respectively.

FIG. 1.  $D_{min}$ ,  $D_{98\%}$ ,  $D_{2\%}$ , and EUD for CTV1 and CTV2 ((a)-(h)); legend (i) for all graphs.



Note: The x-axis of the graphs is the patient index as listed in Table 2. The results should not exceed the solid red line, which indicates the treatment planning constraint (see Table 1).

FIG. 2. Bladder  $V_{70}$  and  $V_{75}$ , as well as Rectal  $V_{75}$  and  $V_{80}$ : ((a)-(d)) for different treatment planning techniques using the initial and verification CT images; legend (e) for all graphs.

#### IV. DISCUSSION

Table 2 shows the different patterns of patient positioning and the consequent inter- and intrafractional change in bony anatomy. The change in bony anatomy results in changes in the path length of the protons and will degrade the optimized dose distribution. Therefore these changes should be minimized in patients for proton and ion therapy. With the help of image-guidance techniques, changes in position or alignment of the pelvic girdle are easily detected and corrected. On the other hand, corrections for rotations in the upper thigh bones with respect to the pelvic girdle are less successful. Such corrections are only performed interfractionally. Nonetheless, both types of motion can be observed intra- and interfractionally. The rotation of the upper thigh bones with respect to the pelvic girdle is usually hindered by the immobilization setup. Meanwhile, if the patient relaxes in the immobilization setup or moves within, changes in the bony anatomy can still be observed. Effective patient immobilization restricts intra- and interfractional motion. The results of our study suggest that a body form provides better fixation than the knee-foot fixation, especially intrafractionally.

Rectal balloons are used to reduce rectal toxicity during treatment and improve patient positioning intrafractionally. However, in two out of three cases, the placement of the rectal balloon was different from the position recorded in the initial planning CT. But as the catheters are not marked or indexed, interfractional displacement in the CC direction is likely to happen.<sup>(17)</sup> The effect of setup errors in the rectal balloon is insufficient dose coverage in CTV1 for both patients 8 and 10. The effect on CTV2 was less significant than on CTV1. This is due to the fact that CTV1 includes both the prostate and the seminal vesicles, while CTV2 includes mainly

the prostate and a less fraction of the seminal vesicles than CTV1. The seminal vesicles are less rigid than the prostate and surround the anterior rectal wall. Hence, the structure of the seminal vesicles deforms in shape with the change in rectal filling, while the prostate mostly suffers translational and rotational shifts. The effect of translation shifts in the prostate itself can be verified and corrected for using the markers. However, the deformation in the seminal vesicles could not be corrected. In this work, the CTV to PTV margin was 0.8 cm around the seminal vesicles. Further expansion of the PTV margin around the seminal vesicles can perhaps ensure interfractional dose coverage of CTV1. The authors also suggest using long rectal balloons with volume capacity over 100 ml in order to stabilize the seminal vesicles. It was also found that multiple field optimizations were less robust than the single field optimization in both patients. In the robustness test of  $D_{\min}$  for CTV1, five plans (3 MF and 2 SF) failed the test with  $D_{\min} < 54.0 \text{ Gy}_{1.1}$ . For CTV2, eight plans (6 MF and 2 SF) failed with  $D_{\min} < 70.2 \text{ Gy}_{1.1}$ . The weights of the spots per field are calculated independently for each field in SF optimization. Hence, the target voxel is irradiated by each field. Thus, if one field is affected by organ motion, the other can possibly recover the dose distribution.

Due to the systematic correction of the isocenter, dose conformity in the CTVs is restored despite large shifts in the prostate positions. However, if the shifts occur intrafractionally, they are not corrected. In most cases, the 3D amplitude of the shift is less than the 0.5 cm CTV to PTV margin despite the long time involved (~5 min). This agrees with the results of Vargas et al.<sup>(11)</sup> In their work, shifts by up to 0.5 cm have small effects of the CTV coverage using a similar CTV to PTV margin. In cases where the shift was larger than 0.5 cm (0.6 cm in patient 5), multiple field optimization plans were not robust. In the case of patient 5, no major changes in bony anatomy were detected (see Table 2). The recorded shift indicates that the target volume simply moved away from the isocenter by 0.6 cm.

In all the plans and verifications, the EUD of CTV1 and CTV2 were always higher than the prescribed dose due to the tight constraints on CTV and PTV values during treatment planning optimization.

Using oblique fields did not have a significant effect on the dose distribution of most patients when compared to bilateral fields. Comparison of  $D_{\min}$  (see Fig.1) shows that SFUD methods were generally more robust than multiple field optimizations. However, the location of the  $D_{\min}$  values is dependent on the deformation of the patient, and is likely to average out during the course of a multifraction treatment series.

## V. CONCLUSIONS

The presented cases demonstrated a range of intra- and interfractional motion expected in prostate cases, and their dosimetric consequences. Interfractional motion can be reduced using accurate patient positioning and image guidance. When large motions were observed, SFUD plans appear more robust than MF plans. Meanwhile, one or more robust proton plans using PBS was found despite the different intra- and interfractional motion patterns and different immobilization setup of the patients.

In ongoing studies, several models of rectal balloons are being tested with respect to repositioning accuracy and robustness of proton plans, and a wider spectrum of field arrangements are being investigated.

## REFERENCES

1. Mayahara H, Murakami M, Kagawa K, et al. Acute morbidity of proton therapy for prostate cancer: the Hyogo Ion Beam Medical Center experience. *Int J Radiat Oncol Biol Phys.* 2007;69(2):434–43.
2. Slater JD, Rossi CJ Jr., Yonemoto LT, et al. Proton therapy for prostate cancer: the initial Loma Linda University experience. *Int J Radiat Oncol Biol Phys.* 2004;59(2):348–52.



3. Zietman AL, Bae K, Slater JD, et al. Randomized trial comparing conventional-dose with high-dose conformal radiation therapy in early-stage adenocarcinoma of the prostate: long-term results from proton radiation oncology group/american college of radiology 95-09. *J Clin Oncol*. 2010;28(7):1106–11.
4. International Commission on Radiation Units and Measurements. *Clinical proton dosimetry*. Bethesda, MD: International Commission on Radiation Units and Measurements; 1998.
5. Mock U, Bogner J, Georg D, Auburger T, Potter R. Comparative treatment planning on localized prostate carcinoma conformal photon- versus proton-based radiotherapy. *Strahlenther Onkol*. 2005;181(7):448–55.
6. Trofimov A, Nguyen PL, Coen JJ, et al. Radiotherapy treatment of early-stage prostate cancer with IMRT and protons: a treatment planning comparison. *Int J Radiat Oncol Biol Phys*. 2007;69(2):444–53.
7. Zhang X, Dong L, Lee AK, et al. Effect of anatomic motion on proton therapy dose distributions in prostate cancer treatment. *Int J Radiat Oncol Biol Phys*. 2007;67(2):620–29.
8. Muzik J, Soukup M, Alber M. Comparison of fixed-beam IMRT, helical tomotherapy, and IMPT for selected cases. *Med Phys*. 2008;35(4):1580–92.
9. Cella L, Lomax A, Miralbell R. Potential role of intensity modulated proton beams in prostate cancer radiotherapy. *Int J Radiat Oncol Biol Phys*. 2001;49(1):217–23.
10. Lomax AJ. Intensity modulated proton therapy and its sensitivity to treatment uncertainties 2: the potential effects of inter-fraction and inter-field motions. *Phys Med Biol*. 2008;53(4):1043–56.
11. Vargas C, Wagner M, Indelicato D, et al. Image guidance based on prostate position for prostate cancer proton therapy. *Int J Radiat Oncol Biol Phys*. 2008;71(5):1322–28.
12. Soukup M, Söhn M, Yan D, Liang J, Alber M. Study of robustness of IMPT and IMRT for prostate cancer against organ movement. *Int J Radiat Oncol Biol Phys*. 2009;75(3):941–49.
13. Hoogeman MS, van Herk M, de Bois J, Lebesque JV. Strategies to reduce the systematic error due to tumor and rectum motion in radiotherapy of prostate cancer. *Radiother Oncol*. 2005;74(2):177–85.
14. Nuver TT, Hoogeman MS, Remeijer P, van Herk M, Lebesque JV. An adaptive off-line procedure for radiotherapy of prostate cancer. *Int J Radiat Oncol Biol Phys*. 2007;67(5):1559–67.
15. D'Amico AV, Manola J, Loffredo M, et al. A practical method to achieve prostate gland immobilization and target verification for daily treatment. *Int J Radiat Oncol Biol Phys*. 2001;51(5):1431–36.
16. van Lin EN, Kristinsson J, Philippens ME, et al. Reduced late rectal mucosal changes after prostate three-dimensional conformal radiotherapy with endorectal balloon as observed in repeated endoscopy. *Int J Radiat Oncol Biol Phys*. 2007;67(3):799–811.
17. van Lin EN, van der Vicht LP, Witjes JA, Huisman HJ, Leer JW, Visser AG. The effect of an endorectal balloon and off-line correction on the interfraction systematic and random prostate position variations: a comparative study. *Int J Radiat Oncol Biol Phys*. 2005;61(1):278–88.
18. Boehmer D, Maingon P, Poortmans P, et al. Guidelines for primary radiotherapy of patients with prostate cancer. *Radiother Oncol*. 2006;79(3):259–69.
19. Meijer GJ, de Klerk J, Bzdusek K, et al. What CTV-to-PTV margins should be applied for prostate irradiation? Four-dimensional quantitative assessment using model-based deformable image registration techniques. *Int J Radiat Oncol Biol Phys*. 2008;72(5):1416–25.
20. van der Wielen GJ, Mutanga TF, Incrocci L, et al. Deformation of prostate and seminal vesicles relative to intraprostatic fiducial markers. *Int J Radiat Oncol Biol Phys*. 2008;72(5):1604–11.
21. Kotte AN, Hofman P, Lagendijk JJ, van Vulpen M, van der Heide UA. Intrafraction motion of the prostate during external-beam radiation therapy: analysis of 427 patients with implanted fiducial markers. *Int J Radiat Oncol Biol Phys*. 2007;69(2):419–25.
22. Niemierko A. A generalized concept of equivalent uniform dose (EUD) [abstract]. *Med Phys*. 1999;26:1100.
23. Tomé WA and Fowler JF. On cold spots in tumor subvolumes. *Med Phys*. 2002;29(7):1590–98.
24. Fu W, Yang Y, Li X, Heron DE, Huq MS, Yue NJ. Dosimetric effects of patient rotational setup errors on prostate IMRT treatments. *Phys Med Biol*. 2006;51(20):5321–31.
25. Wu Q, Mohan R, Niemierko A, Schmidt-Ullrich R. Optimization of intensity-modulated radiotherapy plans based on the equivalent uniform dose. *Int J Radiat Oncol Biol Phys*. 2002;52(1):224–35.